

ORIGINAL ARTICLE

Open Access



Wear Characteristics of the Nuclear Control Rod Drive Mechanism (CRDM) Movable Latch Serviced in High Temperature Water

Tianda Yu^{1,2}, Guozhong Fu², Yanqing Yu³, Liting Zhu³, Maofu Liu⁴, Wei Li¹, Qiang Deng² and Zhenbing Cai^{3*}

Abstract

The current research of nuclear control rod drive mechanism (CRDM) movable latch only makes a simple measurement of wear mass. The wear volume and difference in various claw surfaces are ignored and the degradation mechanism of each claw surface is not clear. In this paper, a detailed degradation analysis was carried out on each claw surface of movable latch combined with wear result and worn morphology. Results indicate that the boundary of carbide is preferred for corrosion because carbide presents a nobler Volta potential compared to the metal matrix or boundary region. Due to the oscillation of drive shaft between the claw surfaces of movable latch, the dominant wear mechanism on the upper surface of claw (USC) and lower surface of claw (LSC) is plastic deformation caused by impact wear. Mechanical impact wear will cause the fragmentation of carbides because of the high hardness and low ductility of carbides. Corrosion promotes the broken carbides to fall off from the metal matrix. The generated fine carbides (abrasive particles) cause extra abrasive wear on USC when the movable brings the drive shaft upward or downward. As a result, USC has a higher wear volume than LSC. This research proposes a method to evaluate the wear on the whole movable latches using a 3D full-size scanner.

Keywords: CRDM, Movable latch, Degradation analysis, Wear characteristics, Carbide

1 Introduction

The control rod drive mechanism (CRDM) is located inside the nuclear pressure vessel, which drives the neutron absorption control rod to move up and down, keeps at the commanding height, and drops when the power is off, thereby completing the reactor startup, power adjustment, and safe shutdown [1, 2]. Nowadays, magnetic lifting CRDM is widely used in a pressurized water reactor. The movable latch, as the key component of magnetic lifting CRDM, is responsible for driving the neutron absorption control rod. The neutron absorption control rod is installed under the drive shaft. The movable latch directly contacts and impacts the drive shaft, resulting in

the tribocorrosion on the movable latch surface in high temperature water [3, 4].

Excessive wear of the latch will affect the action process of CRDM, leading to the occurrence of failure. In general, the Co-based alloy is widely used in nuclear power plant because of its excellent wear resistance and corrosion resistance [5]. The Co element becomes a radioactive source after irradiation and causes radiation damage to materials. Content of Co element is strictly controlled in the nuclear power plant. The movable latch is made of stainless steel substrate and Co-based alloy surfacing layer to improve the service life of CRDM [6]. Besides, C and Cr elements are added to the surfacing layer for enhancement of hardness and corrosion, respectively [7, 8].

In recent years, numerous studies have been carried out on Co-based alloy. Krell et al. [9] reported the sliding wear behavior on various Co-based alloys at an elevated

*Correspondence: czb-jiaoda@126.com

³ Tribology Research Institute, Southwest Jiaotong University, Chengdu 610031, China

Full list of author information is available at the end of the article

temperature and found that the morphology and distribution of carbides had a greater relationship with wear behavior. Nevertheless, the presence of carbides also affects corrosion behavior, especially on the initiation of localized corrosion or dissolution [10]. The carbides in Co-based alloy provide a desirable strengthening technology for wear resistance. However, the boundary of carbides is the preferred location for corrosion due to the Cr depletion at their boundaries [11–13]. The claw surface suffers from the influence of tribocorrosion (the combined action of mechanical wear and corrosion) when the movable latch is exposed to a corrosive environment such as high temperature water [14]. This behavior is no longer a simple superposition of wear and corrosion but a synergistic effect [15]. Wear will cause damage to the passive film and promote corrosion. The generated passive film acts as boundary lubrication to reduce friction and wear [16–18]. Brownlie et al. [19] suggested that wear is the dominant degradation mechanism of the Co-based alloy in the 3.5% NaCl aqueous solution. Wang et al. [20] reported the tribocorrosion behavior on Co-based alloy and found that the fine carbides were broken from the matrix due to the preferred corrosion at the carbides boundary, resulting in abrasive wear. Considering that the movable latch suffers from tribocorrosion behavior, it is necessary to carry out the degradation analysis on the latch surface.

This work is aimed to investigate the wear mechanism of movable latch after 6.5 million steps in high temperature water. A non-contact scanner was used to quantitatively evaluate the wear conditions on each claw surface. Then, the worn morphology was combined with wear results to reveal the degradation mechanism on various claw surfaces.

2 Structural Characteristics of the Movable Latch Assembly

CRDM was fixed above the nuclear reactor core, which drove the movable neutron absorption control rod to move up and down. The main structure of movable latch assembly was composed of lift coil, lift pole, lift armature, movable latch, and drive shaft, as shown in Figure 1. The lift coil was isolated outside the sealed shell and generated a magnetic field after receiving specified instructions. Then, the lift pole attracted the lift armature to move upward. As the movable latch was installed on the lifting armature, the drive shaft moved upward with the movable latch when the lift armature moved upward [21]. The lift armature, movable latch, and drive shaft moved downward under the action of gravity when the lift coil was switched off.

In this process, the movable latch moved a certain distance with the drive shaft and then stopped when

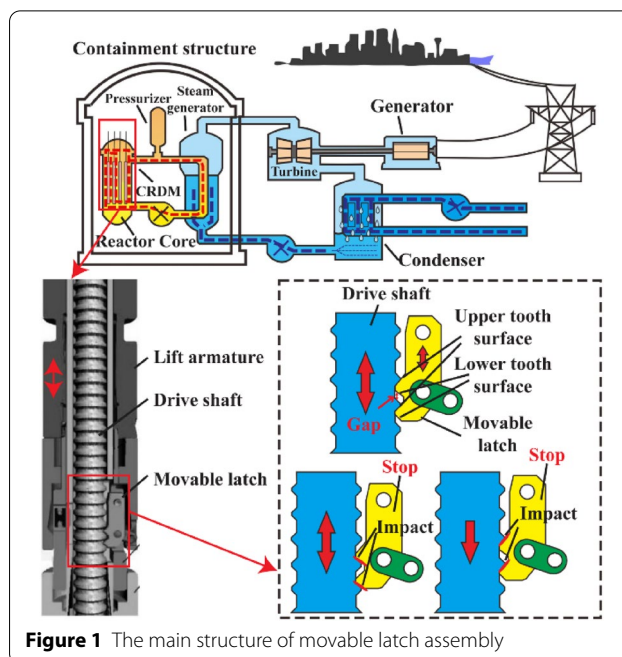


Figure 1 The main structure of movable latch assembly

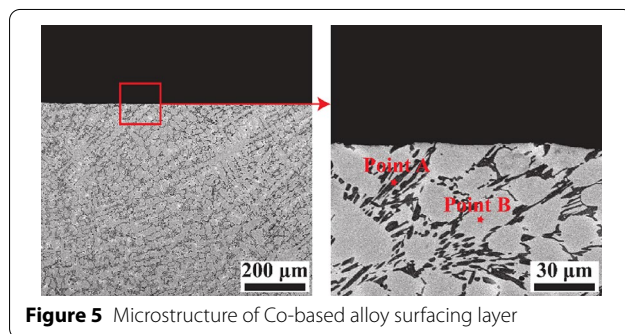
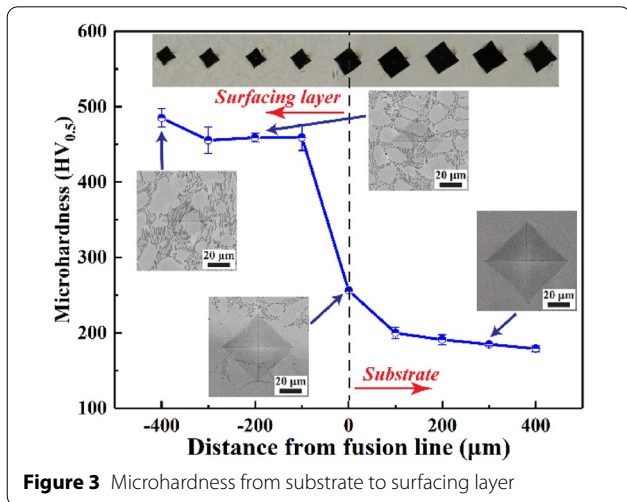
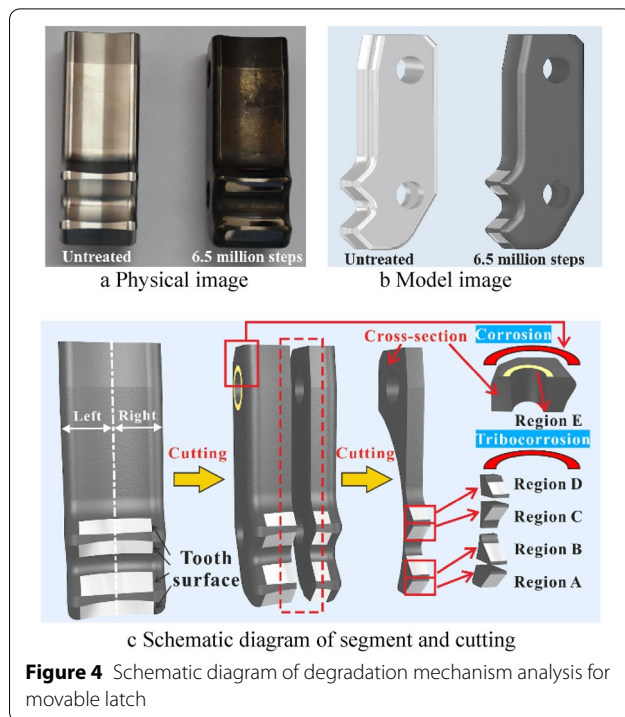
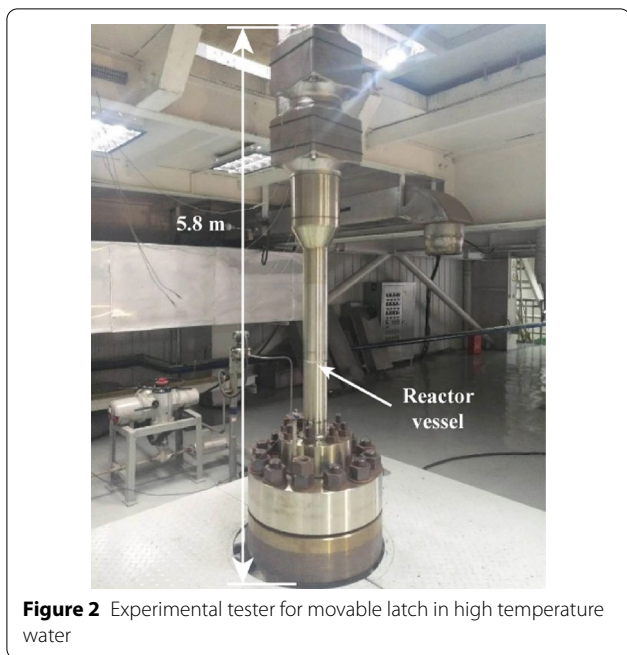
it reached a specified position. Due to the gap between drive shaft and movable latch, the drive shaft oscillated several times between upper surface of claw (USC) and lower surface of claw (LSC) because of inertia effect. The movable latch surface was prone to damage in contact with the drive shaft in high temperature water.

3 Experimental Scheme

To simulate the actual condition of CRDM, the movable latch operated 6.5 million steps in high temperature reactor vessel, which satisfied the design life requirements of 6 million steps [22, 23], as shown in Figure 2. The water temperature and pressure were 300 °C and 15.5 MPa, respectively. The Stellite 6 alloy surfacing layer deposited on austenitic stainless steel substrate was chosen as the sample of movable latch in this work.

Microhardness was measured by a hardness-tester (DHV-1000ZTEST) with a holding time of 10 s and load of 500 g, and the results were shown in Figure 3. Microhardness of substrate was within 179 HV_{0.5} to 200 HV_{0.5}. The scope of surfacing layer was between 455 HV_{0.5} and 485 HV_{0.5}. The microhardness of fusion line between surfacing layer and substrate was equal to 256 HV_{0.5} approximately. The hardness of surfacing layer was 2.5 times that of substrate. The large error bar within the surfacing layer revealed the difference in hardness of various microstructures.

After the experiment, the untreated sample and sample after 6.5 million steps were sprayed developer and scanned with a noncontact 3D full-size scanner



(OKIO-3M-100), as shown in Figure 4a. The model in Figure 4b was obtained using reverse engineering software. The model was segmented and extracted to obtain the wear results including profile, width, depth, area, and volume in various regions. No obvious stress exists on the side of pinhole, which was also composed of Stellite 6 alloy surfacing layer. This region was utilized to analyze corrosion behavior in high temperature water. Accordingly, as shown in Figure 4c, the movable latch was divided into five regions: the claw surfaces (Regions A, B, C, and D) and the side of pinhole

(Region E). The movable latch was cut into blocks using wire cutting for better analysis in various regions.

The surface and cross-sectional morphologies were analyzed with an optical microscope (OM; VHX-7000) and scanning electron microscope (SEM; JSM 7800F) to clarify the degradation mechanism in various regions. X-ray spectroscopy (EDX) and nano-indentation were applied to deeply analyze the microstructure of the precipitates and metal matrix.

4 Experimental Results and Analysis

4.1 Microstructural Characterization

Figure 5 shows the microstructure inside the surfacing layer. The growth of dendrite crystal has a certain orientation but no definite direction. The distribution

Table 1 Chemical composition of precipitate and metal matrix (mass fraction, %)

Element	Co	Cr	Fe	C	Ni	W	Si
Point A	14.2	68.5	0.0	11.8	0.0	3.0	0.0
Point B	60.1	19.4	6.8	4.5	3.6	2.8	1.8

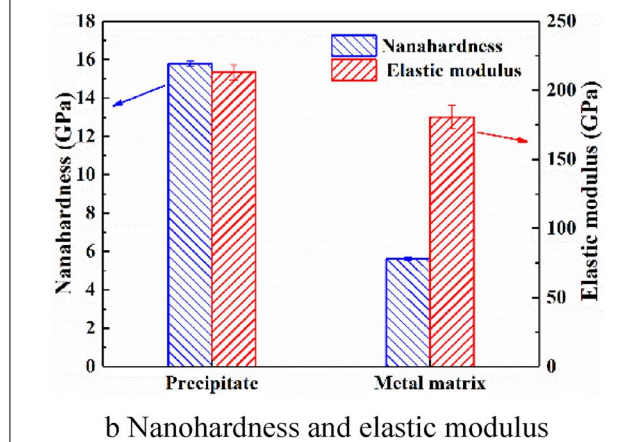
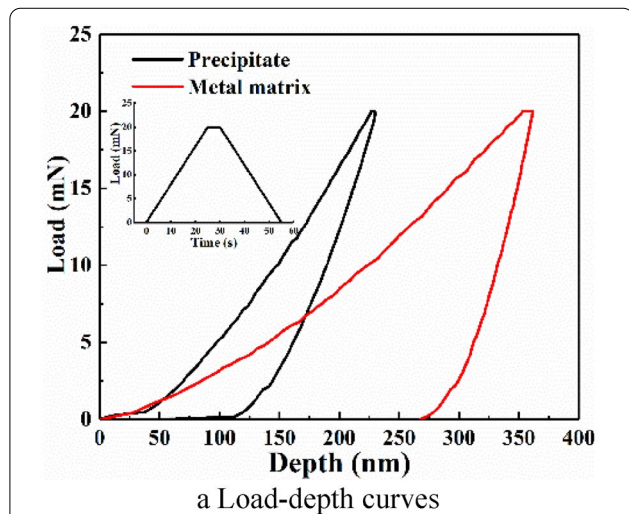
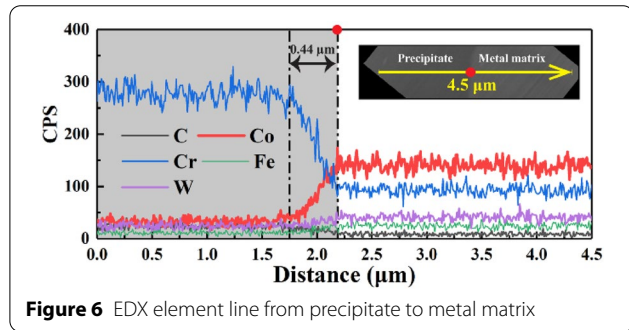
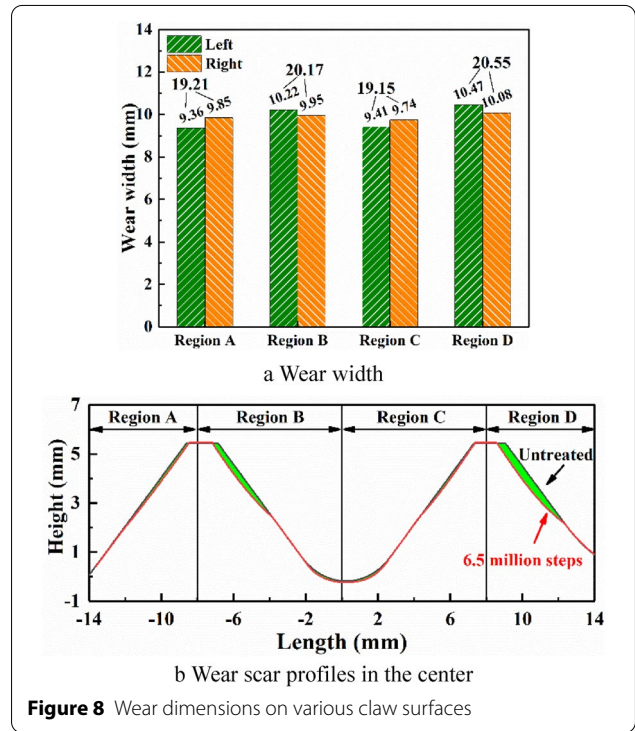


Figure 7 Nanoindentation results of the precipitate and metal matrix



of precipitate (dark particle) and metal matrix (bright region) was displayed through SEM at higher magnification. The large island-like and relatively small dot-scope precipitates are randomly segregated in the grain interior, showing inhomogeneous structures. The chemical composition of precipitate (Point A) and metal matrix (Point B) determined by the point mode EDX technique and is illustrated in Table 1. Results indicate that the precipitates are in rich Cr element, wherein the metal matrix has a relatively low content of Cr element. Meanwhile, the content of C elements within metal matrix is lower than that in the precipitate.

The EDX line scanning result from precipitate to the metal matrix is shown in Figure 6. Same as the point mode EDX results, the dark particles are Cr-rich carbides and the metal matrix is Co-based alloy. At the boundary of carbide, the content of the Cr element declines slowly to the content similar to metal matrix, and this distance is approximately 0.44 μm. This situation is consistent

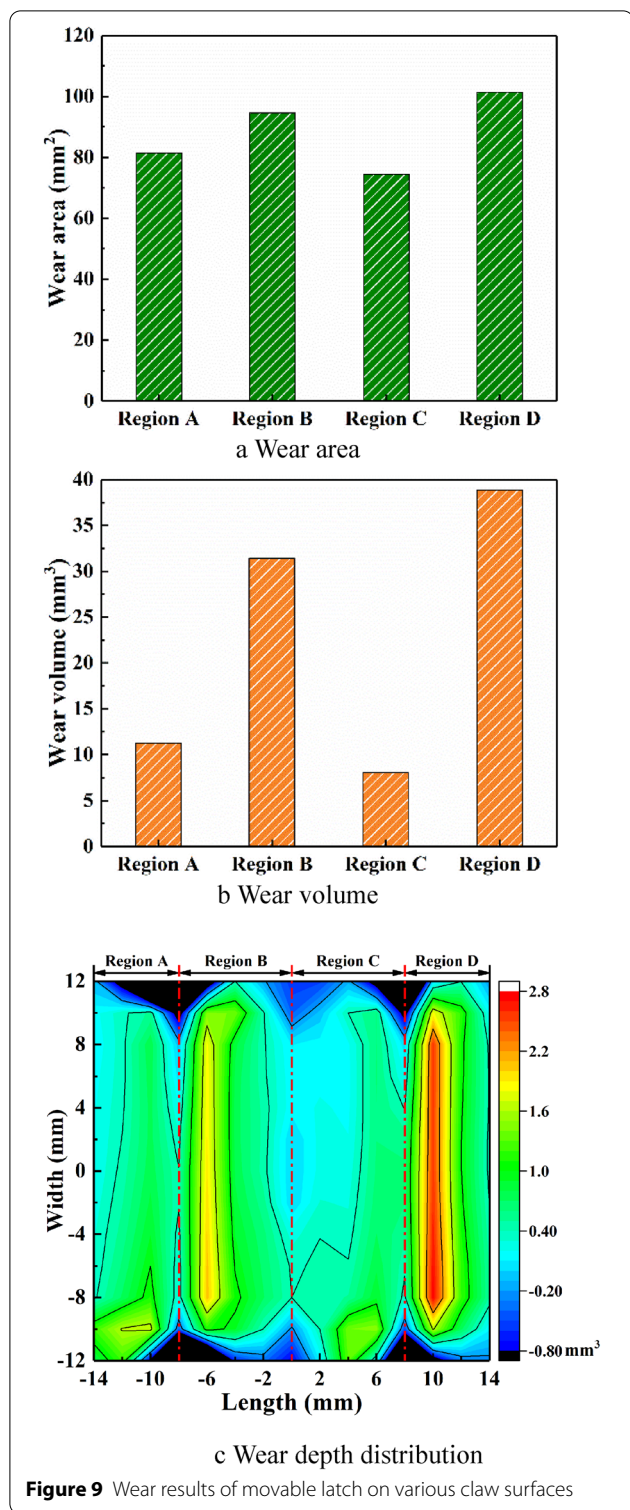


Figure 9 Wear results of movable latch on various claw surfaces

with the studies that the formation of carbides depletes the Cr element at its boundaries [10–13, 24].

Results in Figure 3 present the difference in hardness of various microstructures. The hard phase causes strong

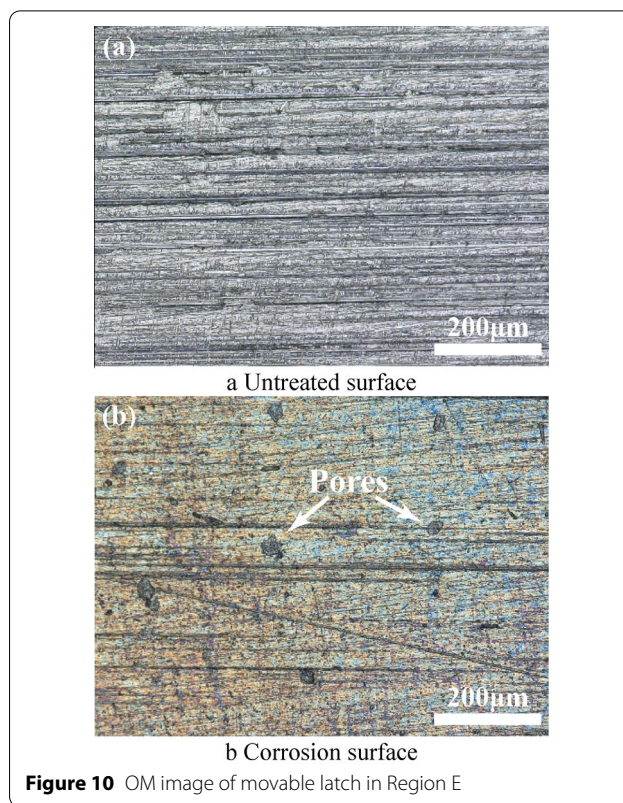


Figure 10 OM image of movable latch in Region E

dispersion hardening within metal matrix [9]. Accordingly, in Figure 7, the nanoindentation experiment is performed on precipitate and metal matrix. In Figure 7a, the maximum depth of metal matrix is deeper than that of precipitate under the same load, which means that the nanohardness of precipitate is higher. The calculated results of nanohardness and elastic modulus in precipitate and metal matrix are shown in Figure 7b. The nanohardness values of precipitate and metal matrix are 15.78 and 5.63 GPa, respectively. The elastic modulus values of precipitate and metal matrix are 212.96 and 180.63 GPa, respectively. Compared to the metal matrix, the nanohardness and elastic modulus of precipitate are increased by 10.15 and 32.33 GPa, respectively. The precipitate has higher hardness and lower ductility [9].

4.2 Wear Results

The wear dimensions on various claw surfaces are shown in Figure 8. On USC (Regions B and D), the wear width on left side is larger than that on right side. The law on LSC (Regions A and C) is the opposite. This situation may be related to the tilt of the movable latch in the running process. Nevertheless, the difference in wear width on various claw surfaces is larger than that on a single claw surface. The USC has higher wear width than LSC.

The total wear width reaches the largest value of 20.55 mm in Region D. Figure 8b shows wear scar profiles at the center of movable latch. Materials removal is found on each claw surface. Same as the wear width, the wear depth on USC is larger than that on LSC.

To better analyze the wear conditions of movable latch on various claw surfaces, wear area, volume, and depth distribution are shown in Figure 9. In Figure 9a, the wear area on USC is higher than that on LSC. The wear volume of each claw surface varies greatly. The wear volume from Region A to Region D is 12.3, 26.3, 9.6, and 37.4 mm³, respectively. The wear volume in Region D is up to four times higher than that in Region C, which indicates more serious wear occurs on USC. The result of wear depth

distribution is counted in Figure 9c for a direct comparison of wear behavior on various claw surfaces. The materials removal between left and right sides is similar for a single claw surface. Material removal on the USC is higher than that on the LSC. As mentioned above, the service behavior on the USC is more complex than that on the LSC, which may be due to the USC suffers extra friction stress [21]. Severe wear will cause a decrease in claw strength [25]. This situation can prove the advantage of double claws because the material removal is shared.

4.3 Worn Morphologies

Figure 10 shows the OM image in Region E to reveal the corrosion behavior on Co-based alloy surfacing layer.

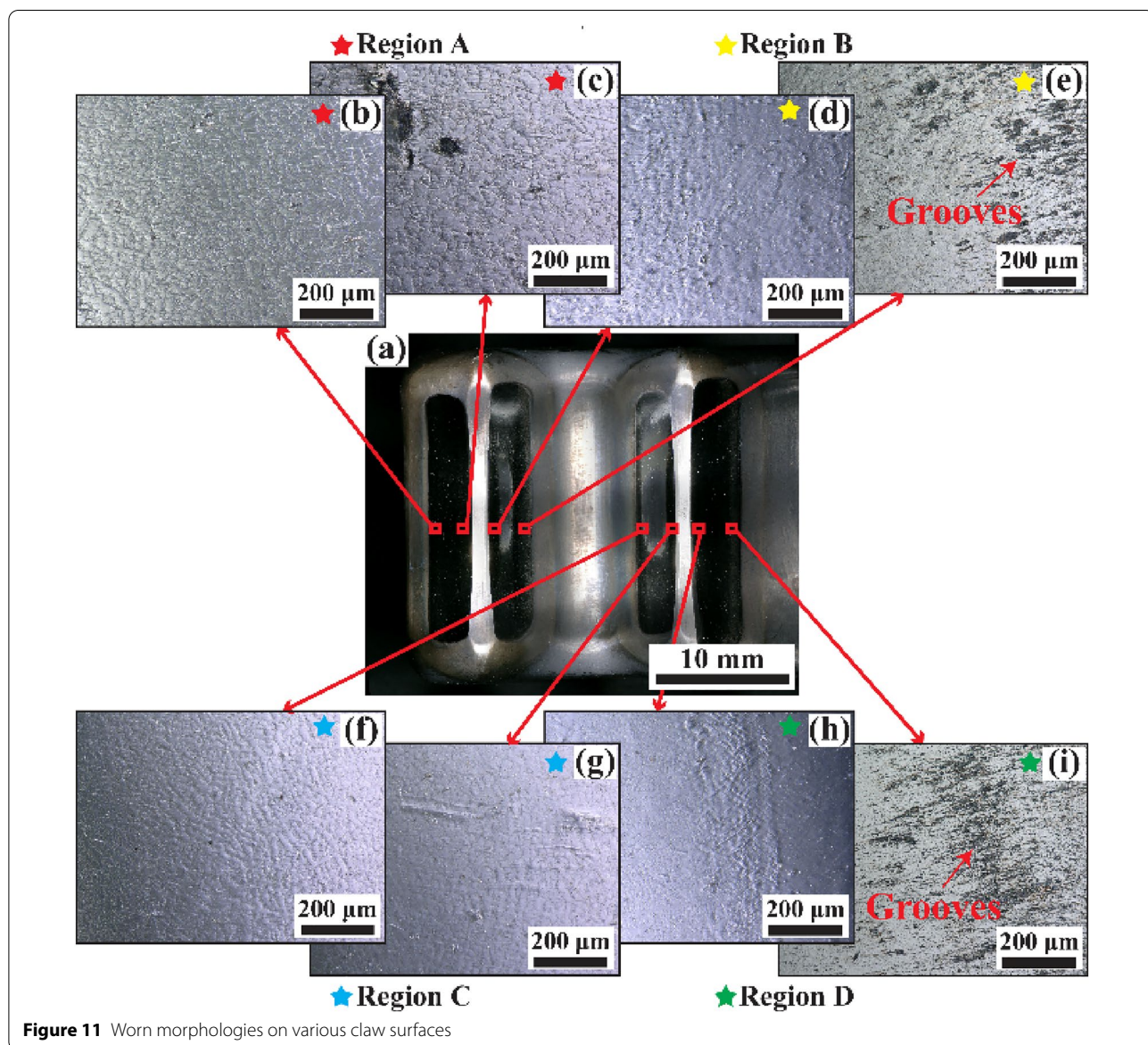


Figure 11 Worn morphologies on various claw surfaces

In Figure 10a, the untreated surface covers the track of machining. Pitting pores are found on the surface of movable latch after 6.5 million steps, as shown in Figure 10b. The falling off of carbides may be responsible for this situation [26, 27].

Figure 11 shows the worn morphologies on each claw surface. The wear scar on LSC is smooth like a polished surface, as previously reported in Ref. [3]. The wear condition on USC is complex compared to LSC. At the top of claw, the wear scar is still smooth. However, multiple wear debris and grooves are found at the root of claw. This situation indicates that the wear mechanism between USC and LSC is different, ultimately leading to the difference in wear volume.

Three typical degradation morphologies of movable latch are shown in Figure 12. The untreated surface has no distinct precipitates, as shown in Figure 12a. The obvious track of machining demonstrates no wear occurs in Region E. Because the boundary of precipitates is preferred for corrosion, the surface in Region E presents the feature of distinctive precipitates with some pitting pores (Figure 12b). Figure 12c shows the typical SEM morphology of LSC. The smooth worn surface indicates the dominant wear mechanism in the low claw is plastic deformation caused by impact wear [28]. Because the hard carbides have low ductility, some cracks can be observed in carbides under the action of cyclic plastic deformation. The typical morphology on USC in Figure 12d presents a severely worn feature. The cracks also exist in the carbides. Besides, grooves and wear debris can be detected on USC, proving abrasive wear occurs on USC.

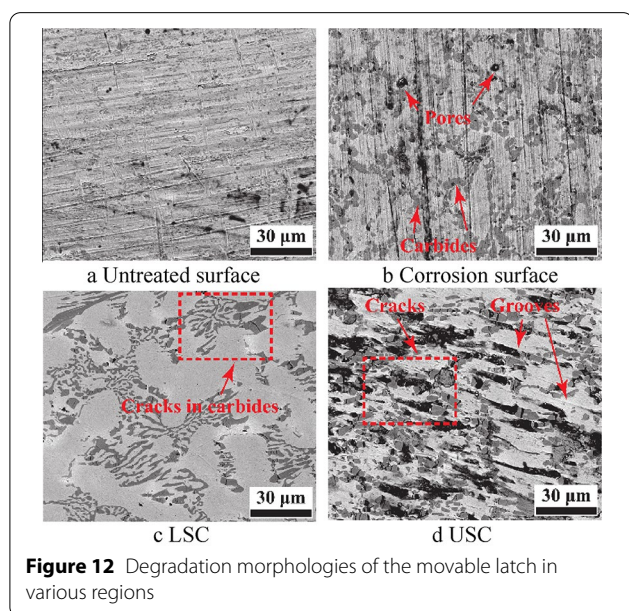


Figure 12 Degradation morphologies of the movable latch in various regions

Figure 13 shows the cross-sectional morphologies in various regions. On the side of pinhole, some cracks are observed from the surface to the inner portion along the boundary of carbides. The fall-off of carbides causes the formation of defects on the surface. On LSC and USC, there are some cracks inside carbides rather than the boundary of carbides. The carbides become smaller particles and fall off from the surface under the combined action of impact wear and corrosion. The material removal causes the defect caused by corrosion is not distinct.

4.4 Analysis of Wear Mechanism

The degradation mechanism of movable latch in various regions is shown in Figure 14. The boundary of carbide is preferred for corrosion because the formation of carbides depletes the Cr element at its boundary [11–16]. A galvanic couple forms between the carbides (cathode) and its boundary (anode). With the increase in corrosion time, the boundary of carbides is almost corroded away and the deeper carbides will be exposed to high temperature water [20]. As a result, in Region E, the crack initiates at the surface and propagates along the carbide boundary to the inner portion. Besides, corrosion also causes the spalling of carbides, resulting in formation of defects and pitting pores [26]. Corrosion only occurs at the surface layer about a few tens of microns after 6.5 million steps, as shown in Figure 13, which indicates the effect of corrosion is slight at high temperature water. However, the corrosion also promotes wear on USC and LSC.

Due to the various operating conditions, the degradation mechanism on USC and LSC are not the same. The LSC mainly suffers impact stress, while USC also suffers friction stress [21]. The dominant wear mechanism on USC is plastic deformation caused by impact wear. The wear scar is smooth like a polished surface (Figure 11). Besides, the cyclic impact will cause the fragmentation of carbides. Because the hard carbides have low ductility [3], the high strain caused by plastic deformation leads to cracks inside carbides (Figure 12c). The broken carbides become smaller and easier to fall off from the surface due to the combined action of corrosion and impact wear. Mechanical impact wear continuously destroys the surface and causes effective material removal, which inhibits the expansion of crack and the formation of large pitting pores. Therefore, there is no crack at the boundary of carbides, and the pitting pores are very small.

The top and root of USC have distinct wear morphology. At the top of USC, the wear scar morphology is similar to LSC (Figure 11). This situation proves the wear mechanism of USC contains plastic deformation caused by the impact wear. When the movable brings the drive

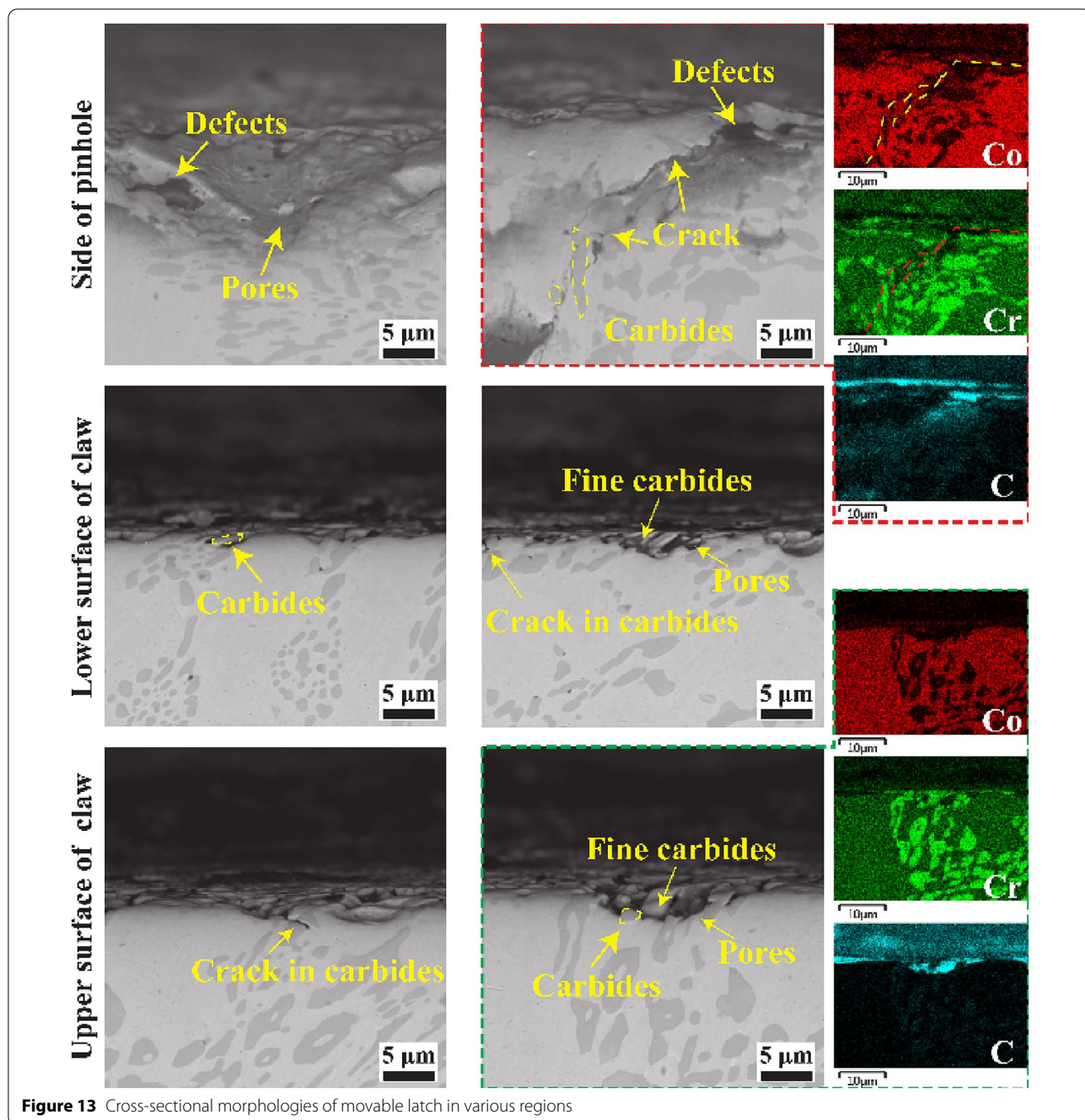


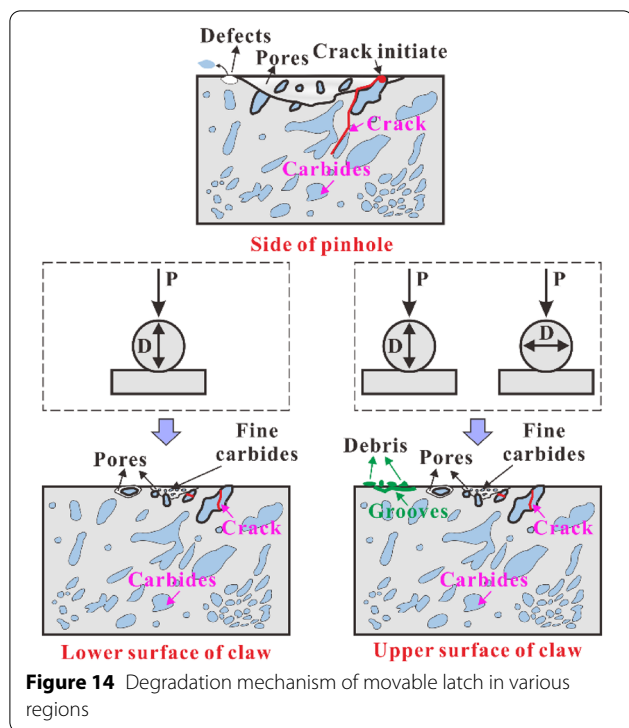
Figure 13 Cross-sectional morphologies of movable latch in various regions

shaft upward or downward for a specified length, the relative movement occurs at the interface between movable latch and drive shaft. A tangential friction pair forms at the interface as the drive shaft has weight. The exfoliated carbides play the role of abrasive particles [29, 30]. Harder carbides erode the surface, leading to the formation of grooves. Accordingly, the USC also suffers abrasive wear, resulting in more serious wear on USC, as shown in Figures 8, 9, 10, 11, 12, 13.

5 Conclusions

Based on a comparative study of the movable latch in various regions, the degradation mechanism of the movable latch serviced in high temperature water was investigated. Thus, the following conclusions were drawn.

- (1) The formation of carbides depletes the Cr element at its boundary and the galvanic couple forms



between the carbides (cathode) and its boundary (anode), leading to the boundary of carbides being preferred for corrosion. The effect of corrosion causes the formation of cracks and pitting pores near the pinhole (Region E).

- (2) Due to the oscillation of drive shaft between the claw surfaces, the dominant degradation in four claw surfaces is plastic deformation caused by impact wear. So the claw surfaces are smooth and look like polished surfaces. Besides, the high strain caused by plastic deformation leads to the fragmentation of carbides.
- (3) Corrosion will cause the broken carbides is easy to fall off from the metal matrix. The generated fine carbides have high hardness, leading to abrasive wear at the interface between the USC and the drive shaft. It is responsible for higher wear volume compared to the LSC.

Acknowledgements

Not applicable.

Authors' Contributions

LZ and WL were in charge of the whole trial; TY and GF wrote the manuscript; YY and ZC assisted with sampling and laboratory analyses. ML and QD assisted in components design and manufacture. All authors read and approved the final manuscript.

Authors' Information

Tianda Yu, born in 1985, is currently an engineer at Nuclear Power Institute of China, China. His main research interests include nuclear power plant reactor structure design.

Guozhong Fu, born in 1987, is currently an engineer at Nuclear Power Institute of China, China. His main research interests include control rod drive mechanism design and development, multi-objective design optimization, and reliability evaluation.

Yanqing Yu, born in 1996, is a PhD candidate at Southwest Jiaotong University, China. He works on fretting wear study.

Liting Zhu, born in 1995, is a master candidate at Southwest Jiaotong University, China. She works on fretting wear study.

Maofu Liu, born in 1986, is currently an engineer at Sichuan Huadu Nuclear Equipment Manufacturing Co., Ltd., China. He works on the processing and manufacturing of nuclear equipment.

Wei Li, born in 1987, is currently an engineer at Nuclear Power Institute of China, China. His main research interests include nuclear power plant reactor structure design.

Qiang Deng, born in 1987, is currently an engineer at Nuclear Power Institute of China, China. His main research interests include the design of nuclear reactor control rod drive mechanism.

Zhenbing Cai, born in 1981, is currently a professor and a PhD supervisor at Southwest Jiaotong University, China. His main research interests include tribology, surface engineering, and the service behavior of key parts of large equipment (high-speed railway, nuclear power, etc.).

Funding

Supported by Sichuan Science and Technology Program (Grant No. 2019ZDZX0001), National Natural Science Foundation of China (Grant No. U2067221), and Sichuan Science and Technology Planning Project (Grant No. 22JQQN0111).

Competing Interests

The authors declare no competing financial interests.

Author Details

¹The State Key Laboratory of Power Transmission Equipment & System Security and New Technology, Chongqing University, Chongqing 4000442, China.

²Science and Technology on Reactor System Design Technology Laboratory, Nuclear Power Institute of China, Chengdu 610041, China. ³Tribology Research Institute, Southwest Jiaotong University, Chengdu 610031, China. ⁴Sichuan Huadu Nuclear Equipment Manufacturing Co., Ltd, Dujiangyan 611830, China.

Received: 16 March 2021 Revised: 15 November 2021 Accepted: 18 February 2022

Published online: 05 April 2022

References

- [1] I G Kim, I C Bang. J. Hydraulic control rod drive mechanism concept for passive in-core cooling system (PINCS) in fully passive advanced nuclear power plant. *Experimental Thermal and Fluid Science*, 2017, 85: 266-278.
- [2] H B Sun, W Q Li, T D Yu, et al. Research on associated motion simulation method and platform of control rod driving mechanism. *Advances in Mechanical Engineering*, 2021, 13(9): 1-16.
- [3] S Guadalupe, C Falcand, W Chitty, et al. Tribocorrosion in pressurized high-temperature water: A mass flow model based on the third-body approach. *Tribology Letters*, 2016, 62(1):10.
- [4] E Lemaire, M L Calvar. Evidence of tribocorrosion wear in pressurized water reactors. *Wear*, 2011, 249: 338-344.
- [5] S Apay, G Behcet. Wear properties of AISI 1015 steel coated with Stellite 6 by microlaser welding. *Materials & Design*, 2014, 55: 1-8.
- [6] D Hertz. Approach to analysis of wear mechanisms in the case of RCCAs and CRDM latch arms: From observation to understanding. *Wear*, 2016, 261: 1024-1031.
- [7] G Cacciamani, G Roncallo, Y Wang, et al. Thermodynamic modelling of a six component (C-Co-Cr-Ni-Ta-W) system for the simulation of Cobalt based alloys. *Journal of Alloys and Compounds*, 2018, 730: 291-310.

- [8] J Y Wang, W H Li, H L Yang, et al. Corrosion behavior of CoCrNi medium-entropy alloy compared with 304 stainless steel in H₂SO₄ and NaOH solutions. *Corrosion Science*, 2020, 177: 108973.
- [9] J Krell, A Röttger, W Theisen. Comprehensive investigation of the microstructure-property relationship of differently manufactured Co–Cr–C alloys at room and elevated temperature. *Wear*, 2020, 444: 203138.
- [10] E Bettini, C Leygraf, C J Lin, et al. Influence of grain boundaries on dissolution behavior of a biomedical CoCrMo alloy: In-situ electrochemical-optical, AFM and SEM/TEM studies. *Journal of The Electrochemical Society*, 2012, 159: C422–C427.
- [11] E Bettini, T Eriksson, M Boström, et al. Influence of metal carbides on dissolution behavior of biomedical CoCrMo alloy: SEM, TEM and AFM studies. *Electrochimica Acta*, 2011, 56: 9413–9419.
- [12] G N Karimi, P H Shipway, D A Stewart, et al. Corrosion of cast Stellite-3 analogue in simulated PWR conditions. *Corrosion Science*, 2018, 140: 402–411.
- [13] Dong, Q Sun, Y N Zhou, et al. Influence of microstructure on corrosion behavior of biomedical Co–Cr–Mo–W alloy fabricated by selective laser melting. *Corrosion Science*, 2020, 170: 108688.
- [14] D Landolt, S Mischler, M Stemp. Electrochemical methods in tribocorrosion: A critical appraisal. *Electrochimica Acta*, 2001, 46:3913–3929.
- [15] S Guadalupe, S Cao, M Cantoni, et al. Applicability of a recently proposed tribocorrosion model to CoCr alloys with different carbides content. *Wear*, 2017, 376: 203–211.
- [16] X R Wang, D G Wang, X W Li, et al. Comparative analyses of torsional fretting, longitudinal fretting and combined longitudinal and torsional fretting behaviors of steel wires. *Engineering Failure Analysis*, 2018, 85: 116–125.
- [17] D G Wang, J Zhang, S R Ge, et al. Mechanical behavior of hoisting rope in 2 km ultra deep coal mine. *Engineering Failure Analysis*, 2019, 106: 104185.
- [18] D G Wang, Z C Zhu, D Z Song. Effects of tensile stress ratio and amplitude on tension-torsion fretting-corrosion-fatigue behaviors of non-perpendicularly crossed steel wires. *Engineering Failure Analysis*, 2020, 117:104839.
- [19] F Brownlie, C Anene, T Hodgkiess, et al. Comparison of Hot Wire TIG Stellite 6 weld cladding and lost wax cast Stellite 6 under corrosive wear conditions. *Wear*, 2018, 404: 71–81.
- [20] Z W Wang, Y Yan, L Xing, et al. The role of hard phase carbides in tribocorrosion processes for a Co-based biomedical alloy. *Tribology International*, 2017, 113: 370–376.
- [21] S T Ling, W Q Li, T D Yu, et al. Analysis and optimization research on latch life of control rod drive mechanism based on approximate model. *Nuclear Engineering and Technology*, 2021, 53:4166–4178.
- [22] T D Yu, J Q Zhang, L Luo, et al. Reliability analysis on compound impact wear of the latch teeth in a control-rod drive mechanism. *Journal of Machine Design*, 2021, 38(4):16–22 (in Chinese).
- [23] F Y Yang, X N Chen, X C Yang. Research on manufacture for ACP 1000 CRDM latch used in Hualong No. 1 plant. *Machine Design and Manufacturing Engineering*, 2017, 46(1):89–93 (in Chinese).
- [24] C V Vidal, A I Muñoz. Effect of thermal treatment and applied potential on the electrochemical behaviour of CoCrMo biomedical alloy. *Electrochimica Acta*, 2009, 54: 1798–1809.
- [25] R P Sekar, R Sathishkumar. Enhancement of wear resistance on normal contact ratio spur gear pairs through non-standard gears. *Wear*, 2017, 380:228–239.
- [26] C Liu, J B Zhao, X Li, et al. Size dependency between the carbides and durability of X80 steel in acid solid environment. *Journal of Electroanalytical Chemistry*, 2020, 873: 114506.
- [27] H Q Yin, Y Y Zhou, Q Liu, et al. Corrosion behavior and mechanism of GH3535 alloy in NaOH, HF and H₂O₂ solution. *Journal of Alloys and Compounds*, 2021, 887: 161387.
- [28] Z B Cai, J F Peng, H Qian, et al. Impact fretting wear behavior of alloy 690 tubes in dry and deionized water conditions. *Chinese Journal of Mechanical Engineering*, 2017, 30: 819–828.
- [29] S Zhou, Y Shen, H Zhang, et al. Heat treatment effect on microstructure, hardness and wear resistance of Cr26 white cast iron. *Chinese Journal of Mechanical Engineering*, 2015, 28: 140–147.
- [30] T Chen, L Song, S Li, et al. Experimental study on wear characteristics of PCBN tool with variable chamfered edge. *Chinese Journal of Mechanical Engineering*, 2019 32: 1–9.

Submit your manuscript to a SpringerOpen[®] journal and benefit from:

- Convenient online submission
- Rigorous peer review
- Open access: articles freely available online
- High visibility within the field
- Retaining the copyright to your article

Submit your next manuscript at ► [springeropen.com](https://www.springeropen.com)
